ASSESSMENT OF RUNOFF COMPONENTS USING GLACIO-HYDROLOGICAL MODEL

M. Tech Thesis

By

Mritunjay Kumar (2302104014)

DEPARTMENT OF CIVIL ENGINEERING

INDIAN INSTITUTE OF TECHNOLOGY INDORE

MAY2025

ASSESSMENT OF RUNOFF COMPONENTS USING GLACIO-HYDROLOGICAL MODEL

A THESIS

submitted in partial fulfilment of the Academic requirements for the award of the degree

of

Master of Technology

by

Mritunjay Kumar (2302104014)

DEPARTMENT OF CIVIL ENGINEERING

INDIAN INSTITUTE OF TECHNOLOGY INDORE

MAY 2025

INDIAN INSTITUTE OF TECHNOLOGY INDORE

CANDIDATE'S DECLARATION

I hereby certify that the work which is being presented in the thesis entitled **Assessment of runoff component using glacio-hydrological model** in the partial fulfilment of the requirements for the award of the degree of **MASTER OF TECHNOLOGY** and submitted in the **DEPARTMENT OF CIVIL ENGINEERING, Indian Institute of Technology Indore**, is an authentic record of my work carried out during the time period from July 2023 to June 2025 under the supervision of Dr. Mohd. Farooq Azam, Associate Professor in the Department of civil engineering, Indian institute of technology, Indore.

The matter presented in this thesis has not been submitted by me for the award of any other degree of this or any other institute.

Mritunjay Kumar
29-05-2025

Signature of the student with date
(Mritunjay Kumar)

This is to certify that the above statement made by the candidate is correct to the best of my/our knowledge.

Mohd. Farooq Azam

Signature of the Supervisor of M.Tech. thesis (with date)
(Dr. Mohd. Farooq Azam) 29/05/2025

Mritunjay Kumar has successfully given his/her M.Tech. Oral Examination held on **24 May 2025.**

Mohd. Farooq Azam

Signature(s) of Supervisor(s) of M.Tech. thesis
Date: 29/05/2025

Convener, DPGC
Date: 31/05/2025

ACKNOWLEDGEMENT

I would like to express my sincere gratitude to all those who supported me throughout the completion of this MTech thesis. First and foremost, I am deeply thankful to my supervisor, Dr. Mohd. Farooq Azam, for his invaluable guidance, encouragement, and insightful suggestions throughout this research. His continuous support and constructive feedback played a crucial role in shaping the direction and quality of this work. I extend my heartfelt appreciation to the faculty and staff of the Department of Civil Engineering, Indian Institute of Technology Indore, for providing the academic environment, resources, and infrastructure essential for conducting this research. Their contributions have been vital to the successful completion of this thesis.

I would especially like to acknowledge the support and mentorship provided by my lab mates at Glacio-Hydro-Climate Lab, Parul Vinze, Md Arif Hussain, Himanshu Kaushik, and Ghulam Hussain, whose guidance and encouragement significantly enriched my learning experience and helped me navigate various stages of this work. I am also grateful to my batchmates for their constant support, cooperation, and for fostering a positive academic atmosphere. Their companionship made this journey more enjoyable, meaningful, and memorable.

Finally, I am forever indebted to my family for their unwavering support, patience, and unconditional belief in me. Their encouragement has been my strength through all the challenges faced during this academic endeavour.

Mritunjay Kumar (2302104014)

Abstract

This study evaluated the runoff components—snow, ice, and rainfall runoff—in the Gangotri glacier system using a glacio-hydrological model from 1980 to 2020. The model was driven using bias-corrected ERA5 reanalysis data for daily air temperature and precipitation extracted from the nearest grid to the Bhojbasa meteorological station. The model was calibrated to get the suitable threshold temperature for melt (Tm) and precipitation gradient (Pg) by minimizing the root mean square error (RMSE) between the available in-situ and modelled runoff for the year 2000-2002, and the model was validated against the available in situ daily runoff data for the year 2003. The study revealed significant interannual variability in runoff, ranging from a minimum of 24.3 m^3/s in 1989 to a maximum of 33.34 m^3/s in 1994, while the mean annual runoff was 29.27 m^3/s over the period 1980-2020. Ice runoff was observed as the primary contributor to the total mean annual runoff, with a 52% contribution, followed by the snow runoff and rainfall contribution of about 36% and 12%, respectively, over the whole period. The pre- and post-2000 period runoff was also estimated to check the impact of increased temperature post-2000, and the increment in runoff was found to be 0.49. The study revealed distinct trends across different temporal intervals because of the various climate variability, highlighting the importance of continuous long-term monitoring to understand the glacier-climate interaction.

TABLE OF CONTENTS

LIST OF FIGURES

LIST OF TABLES

Chapter 1: Introduction

1.1 Glaciers in the Himalaya

A glacier is a large mass of ice that forms from layers of snow over many years and slowly moves downhill under its own weight. They act as natural reservoirs, storing precipitation as snow and ice and gradually releasing it as meltwater. The Himalayan glaciers host more than 42,000 square kilometers of area, making it the largest glacier-covered area outside the polar regions, also coined as the third pole (Nuimura et al., 2015). These glaciers are the headwater sources of major rivers such as the Ganga, Indus, and Brahmaputra, which collectively support more than a billion people in South Asia. These rivers provide essential water for agriculture, drinking, and hydropower, making glaciers essential to both regional water security and livelihood (Azam et al., 2021). Glaciers in the Himalayan region are retreating at an accelerated pace, and this trend is projected to persist in the future under ongoing climatic changes (Nakawo et al., 1997; Hasnain, 1999). The accelerated retreat of Himalayan glaciers poses a serious risk to the livelihoods of millions who rely on glacier-fed water systems. Like other mountain regions, most glaciers in the Himalaya have been receding, primarily due to intensified global warming observed over the last century (Bolch et al., 2012). Glacier runoff plays a critical role in glacier-fed catchments, exerting a strong influence on both the timing and magnitude of streamflow (Singh, Jain, & Shukla, 2021). According to the Sixth Assessment Report by the Intergovernmental Panel on Climate Change (IPCC), glacier runoff is expected to initially increase due to accelerated melting, resulting in greater downstream runoff (Chaturvedi et al., 2022). However, this trend is not indefinite; beyond a certain threshold, often referred to as the "peak water" point-glacier runoff is projected to decline as glacier mass continues to shrink (Huss & Hock, 2018; Nie et al., 2021). One of the most prominent glaciers in the central Himalaya is Gangotri Glacier, located in the Garhwal Himalaya of Uttarakhand, India. Stretching approximately 30 kilometres in length, the glacier feeds the Bhagirathi River, which is a primary tributary of the Ganga River. In the case of the Gangotri Glacier, long-term observations have recorded a total retreat of 819m from 1956-2006. (Bhambri et al., 2012) In addition to glaciers, seasonal snow cover is equally important in the Himalayan hydrological regime, particularly in the context of natural hazards such as avalanches and floods (Bolch et al., 2012). Climate variability has been shown to strongly influence the spatial and temporal

distribution of snow cover, adversely affecting snow runoff and the overall glacier mass balance (Singh, Jain, & Goyal, 2021). Given its crucial role in sustaining river flow and regional climate, the Gangotri Glacier has been widely studied. However, recent signs of accelerated retreat due to rising temperatures and changing snowfall patterns have raised serious concerns about the future availability of water in the Ganga basin.

1.2 Importance of Glacio-Hydrological Modelling

A comprehensive understanding of changing runoff patterns in glacierized and non-glacierized catchments requires more than just observational data. Field measurements are often limited due to difficult terrain, limited accessibility, and weather constraints. To overcome these challenges, glacio-hydrological models have become essential tools. These models simulate the generation and routing of meltwater by incorporating various inputs such as temperature, precipitation, glacier area, and elevation.

Such models are useful for:

- Estimating the contribution of snow runoff, ice runoff, and rainfall to total runoff
- Simulating seasonal and interannual variability in flow
- Predicting how runoff patterns may shift under future climate scenarios

Quantifying the contribution of different hydrological components in the Himalayan River systems has been a key focus in recent research. Several methods have been used for this purpose, including empirical relationships between precipitation and runoff (Thayyen & Gergan, 2010), ice ablation models (Racoviteanu et al., 2013), and chemical tracer techniques (Racoviteanu et al., 2013; Rai et al., 2016). The glaciological method, which relies on direct field-based measurements of glacier mass balance, has also provided critical insights into glacier melt contribution (Kääb et al., 2012; Gardelle et al., 2013). However, due to limited field data and the complexity of glacierized catchments, glacio-hydrological models have emerged as essential tools for understanding runoff dynamics. These models, both semi-distributed and fully distributed, integrate meteorological and glaciological inputs—such as temperature, precipitation, glacier extent, and elevation—to simulate meltwater generation and runoff routing. Recent applications of these models in the Himalayan region include studies by Immerzeel et al. (2013), Nepal et al. (2014), Li et al. (2015), and Chen et al. (2017). Among the various approaches, glacio-hydrological models

are particularly valuable for their ability to assess current hydrological regimes and to project future runoff patterns under climate change scenarios

Glacier hydrology is complex because it involves many factors, such as how glaciers move and melt, climate conditions, and the features of the surrounding area. These factors interact in ways that make it difficult to predict runoff, but it is essential for accurate modelling. Factors such as debris cover, topographic variation, and data limitations introduce uncertainty in model outputs. For reliable predictions, models must be carefully calibrated and validated against observed data to accurately represent melt processes and river runoff.

1.3 Research Motivation and Knowledge Gap

Although multiple studies have examined glacier dynamics and retreat trends in the Gangotri basin, relatively few have focused on the glacier system's hydrological response (Singh et al., 2022; Agarwal et al., 2018; Bhambri et al., 2012), especially in terms of runoff component separation (rain, snow, ice). Furthermore, limited efforts have been made to compare runoff behaviour pre- and post-2000. This study aims to fill this gap by analyzing long-term runoff data, using a glacio-hydrological model, and examining how the contributions of different melt sources to total runoff have changed over time. The goal is to better understand seasonal and decadal variations in runoff from the Gangotri Glacier and their linkages to climatic drivers.

1.4 Objectives of the Study

The objectives of this study are:

1. To examine the total runoff and its primary components—rainfall runoff, snow runoff, and ice runoff—from the Gangotri Glacier basin.
2. To assess and compare runoff dynamics between the pre- and post-2000 periods using the Glacio-Hydrological model.
3. To examine the historical trends of runoff components and quantify the seasonal and interannual contributions of distinct meltwater sources to the overall basin runoff.
4. To evaluate the sensitivity of glacier-fed runoff to climatic variability, providing insights into the hydrological response of the catchment under observed climate trends.

Chapter 2: Literature Review

The Gangotri Glacier has been widely studied because of its crucial role in feeding the Bhagirathi River. Over the past two decades, extensive research has focused on the hydrological significance and mass balance changes of Himalayan glaciers, especially the Gangotri Glacier. Azam et al. (2021) conducted a large-scale assessment of glaciohydrology in the Himalaya-Karakoram region, emphasizing the critical role of snow and ice melt in dry-season runoff across major South Asian River basins like the Indus, Ganges, and Brahmaputra. In a catchment-scale study, Azam et al. (2019) employed a glacio-hydrological model to quantify contributions of snow, ice, and rainfall to total runoff in the Chhota Shigri basin, revealing how climate variables influence melt-driven runoff over decades. Similarly, Singh et al. (2005) explored the hydrological dynamics of the Gangotri Glacier by analyzing runoff variability, storage effects, and melt delay characteristics based on in situ monitoring. Bhambri et al. (2018) reported that the glacier has retreated by about 1000 meters over the last 100 years, mainly due to rising temperatures and changes in precipitation patterns, which have enhanced melting and led to a negative mass balance. Singh et al. (2024) used both field observations and remote sensing data and similarly found that the Gangotri Glacier is experiencing a negative mass balance, largely because of accelerated melting linked to warming temperatures. Some surrounding tributary glaciers, such as Chaturangi and Raktavaran, show contrasting behaviour, with some positive mass balance trends, possibly because of their higher accumulation zones and thicker debris covers. However, the main Gangotri Glacier has continued to retreat significantly, with its snout receding at an average rate of about 18 meters per year (Hussain et al., 2022). Azam and Srivastava (2020) used a temperature-index model to simulate mass balance and runoff for nearby Dokriani Glacier, highlighting the contrasting roles of precipitation and temperature on runoff variability. Singh et al. (2023) adopted GlabTop2 and SPHY models to assess recent changes in Gangotri Glacier's thickness and runoff between 2011–2020, linking thinning trends with altered runoff seasonality. Additional studies by Gantayat et al. (2017) estimated ice thickness in Gangotri Glacier using surface velocity and slope correlations, aiding in hazard assessment and mass estimation. Meanwhile, Bhambri et al. (2012) tracked Gangotri's frontal recession from 1965 to 2006 via satellite, noting slowed retreat in recent years, possibly due to increasing debris cover. Remote sensing studies by Bhambri et al. (2018) and Vishwakarma et al. (2022) have been critical in monitoring changes in the glacier's area and volume over time. These studies have provided important baseline data to understand the impact of climate change on glacier dynamics.

For understanding glacier runoff, hydrological modelling has become an essential tool, especially under changing climatic conditions. Azam et al. (2019) reconstructed the mass balance and runoff of the Chhota Shigri Glacier using a temperature-index model and showed that glacier melt contributed more than half of the annual runoff, with clear seasonal variation linked to temperature changes. Similarly, Immerzeel et al. (2012) applied a cryospheric–hydrological model in the Langtang catchment of Nepal. They found that snow and glacier melt together contributed up to 70% of the dry-season streamflow, highlighting the importance of meltwater for sustaining river flows. Shea et al. (2015) also demonstrated, using an energy balance model in the Everest region, that glacier melt is very sensitive to surface characteristics like debris cover and elevation, and that including radiation components is critical for accurate melt modelling. In terms of runoff modelling, Arora et al. (2024) utilized the HBV hydrological model for Gangotri Glacier, revealing snowmelt as the dominant streamflow contributor, followed by glacier melt and rainfall. The model demonstrated strong calibration and validation performance, stressing the seasonal importance of snow-fed runoff under current climate conditions. Agrawal et al. (2018) combined mass balance and velocity modelling to estimate glacier response to changing precipitation and temperature patterns, linking reduced snowfall to increased runoff. Singh et al. (2024) used remote sensing techniques to analyze Gangotri Glacier's dynamics over two decades, finding mass loss, reduced surface velocity, and accelerated melt due to rising temperature and black carbon deposition. Furthermore, Azam et al. (2016) investigated the long-term meteorological and mass balance patterns of Chhota Shigri Glacier, indicating monsoon snowfall as a crucial driver of interannual mass balance variations.

Although previous studies have provided valuable insights into glacier retreat, mass balance, and meltwater contributions, a major gap still exists in fully understanding the seasonal separation of runoff components (rainfall, snow runoff, ice runoff) specifically for the Gangotri Glacier basin. While mass loss and surface changes have been well-documented, fewer studies have focused on how different climate variables (temperature, precipitation) separately affect rain runoff, snow runoff, and ice runoff. Furthermore, very few studies have applied hydrological modelling specifically to separate and quantify seasonal runoff contributions from the Gangotri Glacier under changing climatic conditions. Addressing this gap is important for better predicting future water availability and managing the region's critical water resources. Moreover, fewer studies have focused on assessing pre- and post-2000 melt dynamics across

different runoff components in Gangotri Glacier, representing a crucial research gap for future hydrological forecasting.

Chapter 3: Study Area

The Gangotri Glacier System (GGS), located in the central Himalaya, is among the largest glacier systems in the Indian Himalaya. It comprises several tributary glaciers (which were part of the system), including Chaturangi, Raktavaran, and Meru, which collectively contribute to the Bhagirathi River, a primary tributary of the Ganga. Among all the tributary glaciers, Gangotri Glacier is the largest having area of 551.37 km^2 and approximately 32 km long and a varied width of 1 to 3 km. The Gangotri Glacier also holds significant religious importance, with its snout called Gaumukh because it resembles like cow's mouth. The glacier originates near the Chaukhamba massif, flows in the southeast direction, and terminates at the Gaumukh, which is located at an elevation of around 3,900 meters above sea level (Figure 1). The glacier flows in a northwest-to-southeast direction and drains into the Bhagirathi River, which later merges with the Alaknanda River at Devprayag, forming the Ganga River, one of the most vital river systems in South Asia.

The glacier has a significant debris cover, accounting for 24% of its total area. It contains numerous ice cliffs and glacial lakes concentrated in the lower ablation zone, which significantly influence melt rates by enhancing the local melt. The glacier's catchment area includes a combination of glacial ice, snowfields, rock outcrops, and seasonal snow, making it a complex system for hydrological modelling.

Table 1: Key geographical and physical characteristics of the GGS, including spatial extent, elevation range, glacierized and non-glacierized areas, and major tributaries contributing to the main glacier system.

Latitude & Longitude	30°43′N-31°01′N & 79°00′E-79°17′E
Glacier Length	~32km
Elevation Range	4000-6950m a.s.l.
Glacierized Area	252.85 Km^2
Non-Glacierized Area	298.53 Km^2
Main tributaries	Chaturangi, Raktavaran, and Meru

The outline of the Gangotri Glacier was extracted from the Randolph Glacier Inventory (RGI version 4), while the catchment boundary was delineated using the Digital Elevation Model (DEM) derived from the Shuttle Radar Topography Mission (SRTM) dataset.

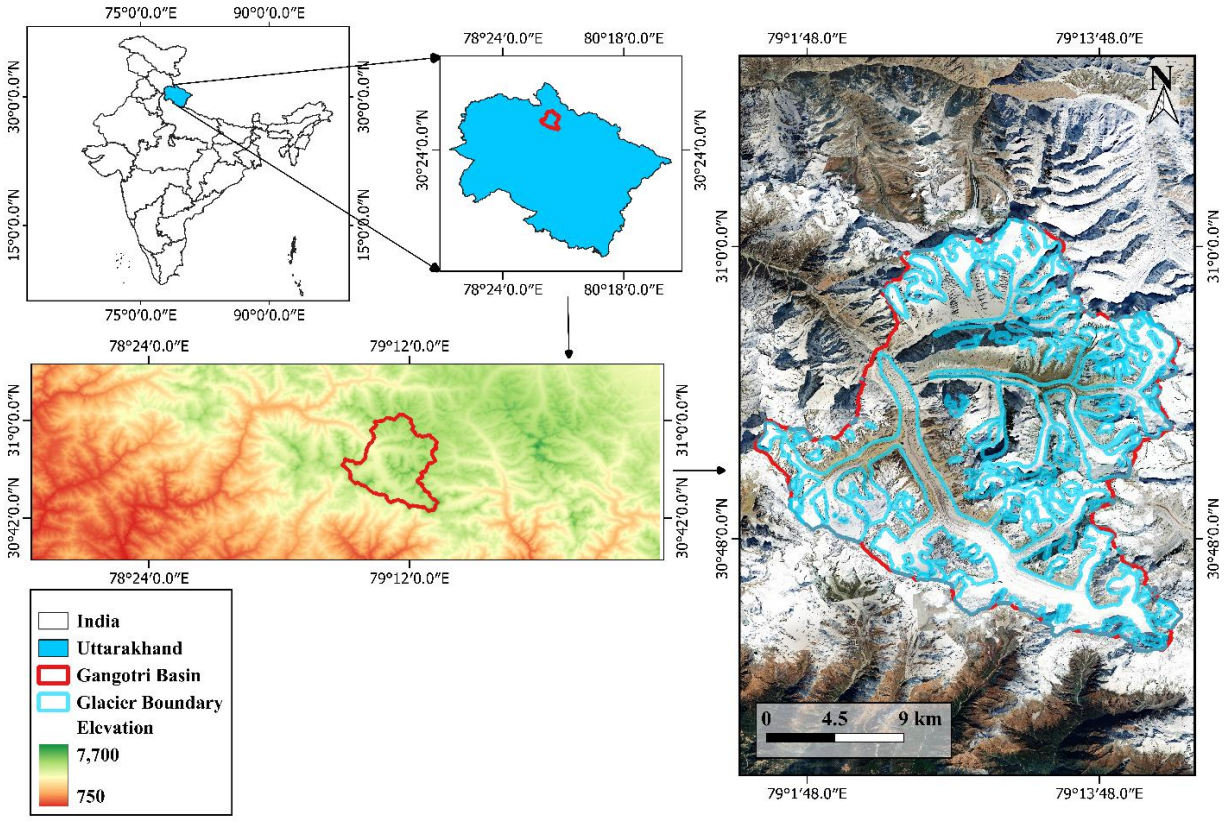

Figure 1: Map showing location of the study area with the Gangotri Glacier system.

3.1 Data, bias correction, and climatic conditions

The reanalysed ERA5 precipitation and temperature (0.25° × 0.25° spatial resolution) were downloaded from the Copernicus Climate Data Store (Hersbach et al., 2020) over the period 1979–2020 for the nearest grid point (30.9505° N, 79.0514° E) of Bhojbasa Base Camp (3,800 m a.s.l), where in-situ Precipitation and Temperature were available. Before using the data in the model, these reanalysed P and T were bias-corrected using the available in-situ P (May 2000 - Oct 2003) and T (May 2006- April 2007) from Singh (2006) and Agrawal (2018). The correction factors were obtained as 0.42 and 1.12 for P and T using linear regression. These correction factors were applied for the whole period. The region's climate, influenced by both the Indian Summer Monsoon (ISM) and Western Disturbances (WD), results in seasonal precipitation and temperature patterns, with rainfall in summer and snow in winter, while the melt of snow and ice from the GGS plays a crucial role in sustaining river flow, especially during the dry months.

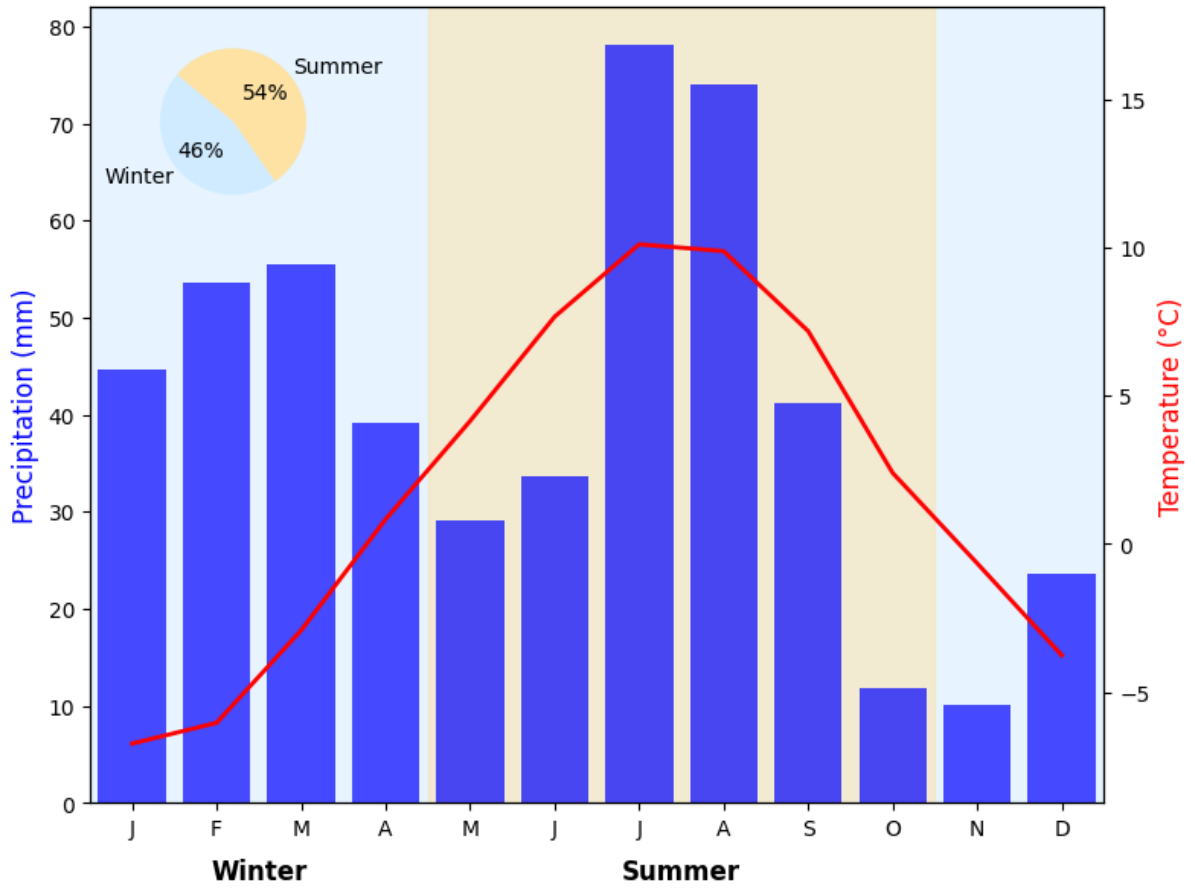

Figure 2: Climate of the Bhojbasa. The blue bars represent the mean monthly precipitation over 1980–2020. The red line represents the mean monthly temperature over 1980–2020. The pie chart represents the % distribution of precipitation in different seasons.

GGS receives nearly equal precipitation contributions from the (ISM) and (WD), with summer (May–October) and winter (November–April) seasons contributing approximately 54% and 46% of the annual total precipitation, respectively (Figure 2). It is important to note that the temperature and precipitation data used here are recorded at Bhojbasa, which is located downstream of the Gangotri Glacier. During the winter months (November–April), the region experiences sub-zero temperatures and moderate precipitation, mostly as snowfall. The average monthly precipitation in this period is about 37.7 mm. In contrast, the summer season (May–October) is influenced by the Indian Summer Monsoon, with temperatures peaking around 10°C in July and monthly precipitation averaging 44.7 mm. The highest rainfall occurs in July and August, aligning with the core monsoon months.

Chapter 4: Methodology

4.1 Glacio-Hydrological Model

To estimate catchment-wide runoff, a glacio-hydrological model (Azam et al., 2019; Srivastava and Azam, 2022) was employed, which integrates three key modules: snow runoff, ice runoff, and rainfall runoff. The model operates on a daily time step and performs calculations across 50-meter elevation intervals throughout the catchment. The model is driven by bias-corrected ERA5 daily precipitation and temperature. To generate spatially distributed input fields, altitudinal gradients in precipitation and temperature lapse rates are applied for each day of the year, following the methodology of Azam et al. (2014a). Simulations are carried out for each hydrological year (from 1st November 1979 to 31st of October 2020), with runoff being calculated for each band by summing contributions from snow runoff, ice runoff, and rain runoff.

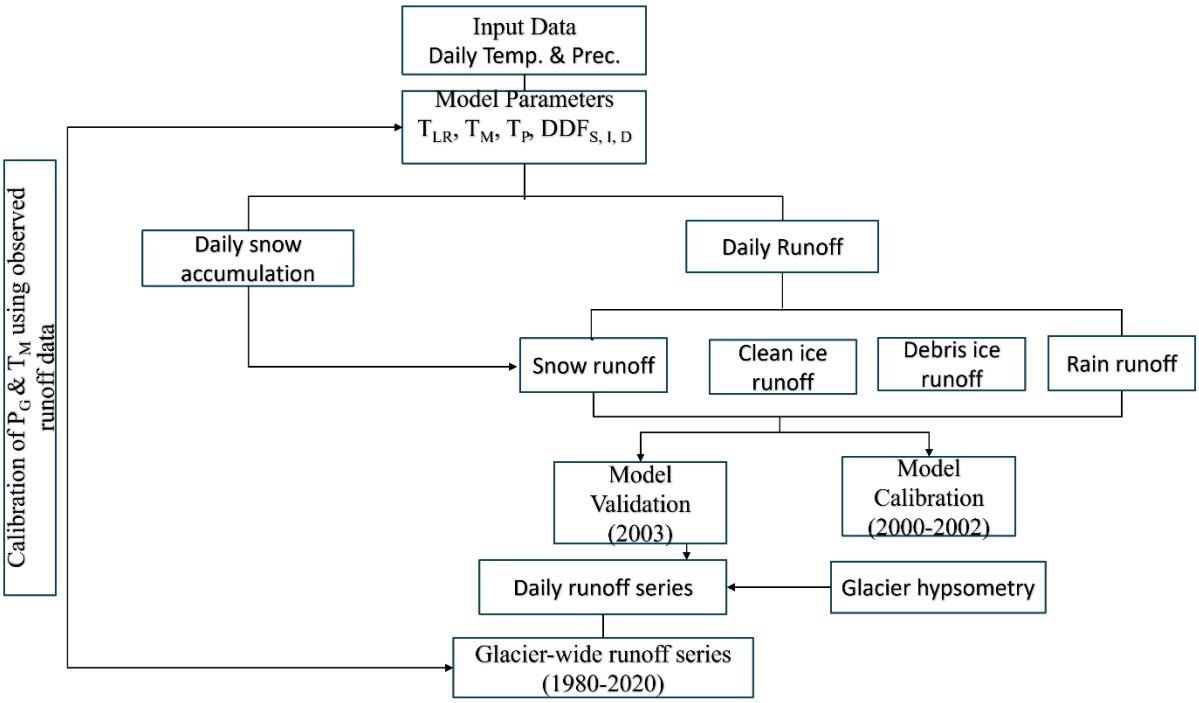

Figure 3 : Runoff model structure.T_P, P_G, T_{LR}, T_M, $DDF_{S, I, D}$ are the threshold temperatures for snow/rain limit, altitudinal precipitation gradient, temperature lapse rates, threshold temperature for melt, degree day factor (DDF) for snow, ice, and debris-covered ice, respectively.

Daily precipitation and temperature data were extrapolated across each 50-meter elevation band using the altitudinal precipitation gradient (P_G) and temperature lapse rates (LRs), respectively.

$$P = P_I + P_G X \Delta H \quad (1)$$

Where P represents the estimated precipitation at a specific elevation band, P_I is the measured precipitation at the base camp (Bhojbasa), and ΔH denotes the elevation difference (in meters) between the base camp and the target elevation band. The precipitation gradient (P_G), expressed as a percentage change per 1000 meters of elevation.

$$T = T_I - LR\Delta H \quad (2)$$

Where T is the calculated temperature at different altitudinal bands, T_i is the temperature at Bhojbasa Base Camp, ΔH is the altitudinal difference between the base camp and corresponding altitudinal band (m), and LR is the monthly lapse rate (°C km^{-1}).

The daily accumulation c (mm w.e.d^{-1}) at each altitudinal range (glacierized and non-glacierized) is computed by:

$$A = \begin{cases} P, & when\ T \leq T_P \\ 0, & when\ T > T_P \end{cases} \quad (3)$$

Where P and T are daily precipitation (mm) and temperature (°C), respectively, extrapolated at glacier elevations, and T_P is the threshold temperature for snow-rain (°C).

The daily accumulation (c) is estimated by using the threshold temperature for snow/rain (T_P), and the daily ablation (A) is estimated by using the threshold temperature for melt (T_M). Snow accumulation occurs when $T < T_P$, and if $T > T_P$, all the snow is melted.

At a given altitudinal range (glacierized and non-glacierized), the daily rainfall is computed using the following equation

$$r = \begin{cases} 0, & whenT \leq T_P \\ P, & whenT > T_P \end{cases} \quad (4)$$

The temperature-index model estimates melt by linking it to the accumulation of positive air temperatures, known as positive degree days, using a proportionality factor referred to as the degree-day factor (DDF)

At each altitudinal range, the ablation A is computed by:

$$A = \begin{cases} DDF_{S,I,D} \,.\, (T - T_M) \;, & when\ T > T_M \\ 0, & when\ T \leq T_M \end{cases} \quad (5)$$

Ablation is estimated by comparing the air temperature with the threshold temperature and applying appropriate degree-day factors (DDF) for different surface conditions such as snow, clean ice, and debris-covered ice.

Total snow runoff (Q_{snow}) over the whole catchment is computed as:

$$Q_{SNOW} = A_{smg} + A_{smng} \quad (6)$$

A_{smg} and A_{smng} are snow runoff over the glacierized and non-glacierized areas, respectively.

Total rainfall runoff Q_{rain}, over the whole catchment, is computed as:

$$Q_{RAIN} = r_g + r_{ng} \quad (7)$$

where r_g and r_{ng} are rainfall runoff from the glacierized and non-glacierized areas, respectively.

The daily runoff, Q_{TOTAL}, at the catchment outlet is finally computed using the following equation:

$$Q_{TOTAL} = Q_{SNOW} + Q_{ICE} + Q_{RAIN} \quad (8)$$

Where, Q_{TOTAL} represents the total runoff, while Q_{SNOW}, Q_{ICE}, and Q_{RAIN} denote the contributions from snowmelt, ice melt (including both clean and debris-covered ice), and rainfall, respectively, across the entire catchment. The ice runoff component (Q_{ICE}) corresponds directly to the ablation from clean and debris-covered ice surfaces.

4.2 Model Parameter

Most of the model parameters were adopted from Hussain et al (2022). DDF was assigned separately for snow and glacier ice to simulate melt, with ice typically having a higher DDF due to lower albedo. A threshold temperature was used to differentiate between rainfall and snowfall and initiate melt processes. Since direct in situ Degree Day Factors (DDFs) for snow, ice, and debris-covered ice are unavailable for the Gangotri Glacier System, values of 6.1 mm d^{-1} $°C^{-1}$ for snow, 7.7 mm d^{-1} $°C^{-1}$ for ice, and 4.8 mm d^{-1} $°C^{-1}$ for debris-covered ice have been adopted. These values were estimated by Azam and Srivastava (2020) based on prior field observations from the Dokriani Bamak Glacier, which is located about 30 km west of the Gangotri Glacier System (Singh et al., 2000; Pratap et al., 2015). The threshold temperature (TP) has been set at 0.7°C, as Jennings et al. (2018) suggested, corresponding to relative humidity levels between 70% and 80% for GGS.

Table 2: Model parameters

Parameters	Model Value	Range
DDF for debris-covered ice (mm $d^{-1}°C^{-1}$)	4.5	–
DDF for ice (mm $d^{-1}°C^{-1}$)	7.7	–
DDF for snow (mm $d^{-1}°C^{-1}$)	6.1	–
Altitudinal precipitation gradient Pg(%km^{-1}) *	88	0 to 100
Threshold temperature for melting (T_M) *	-2.45	-5 to 5

*Calibrated parameters

4.3 Model Calibration

Model calibration is a critical step to ensure that simulated outputs accurately reflect observed glacier mass and runoff dynamics. In this study, two parameters were selected for calibration: the precipitation gradient (P_g) and the melt threshold temperature (T_M). The choice of P_g is particularly important because of the limited availability of in situ precipitation data in the complex Himalayan terrain, which makes spatial precipitation distribution over glacier surfaces highly uncertain. Similarly, T_M is the most sensitive parameter to the melt models (Azam et al., 2019). While melting is typically expected at temperatures above 0°C, several studies have shown that melt can occur even below freezing (Kuhn 1987, Hook,2003).

To calibrate the model, P_g and T_M were systematically varied within physically reasonable ranges of 0% km^{-1} to 100% km^{-1}, and from -5°C to +5°C, respectively. A Monte Carlo simulation approach was adopted, performing 10,000 model runs with different parameter combinations. The model performance was evaluated by comparing the modelled runoff with observed runoff data available for the Gangotri Glacier System during the period 2000–2002 (Singh et al., 2005; Haritashya et al., 2005). The root mean square error (RMSE) between simulated and observed runoff was minimized to identify the optimal parameter set.

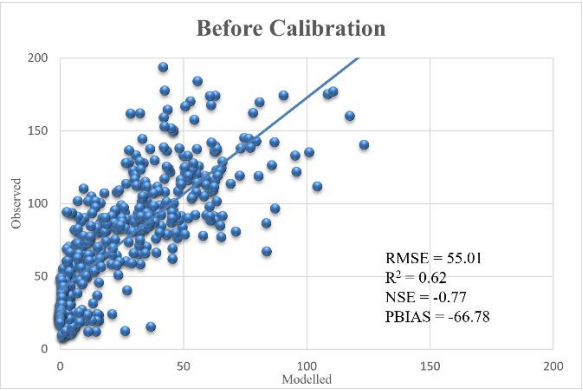

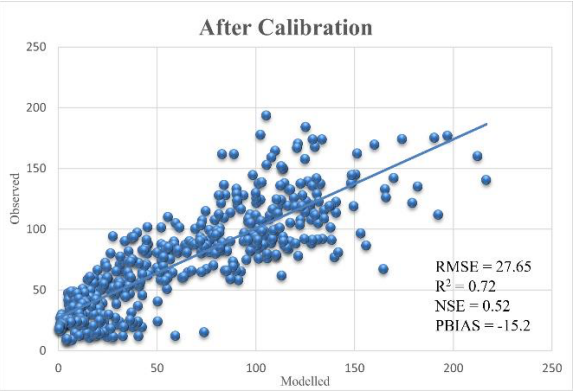

Figure 4: Comparison of modelled and observed runoff before and after calibration for the GGS. The left panel shows model performance before calibration, and the right panel shows after calibration. Each plot includes the coefficient of determination (**R^2**), root mean square error (**RMSE**), Nash–Sutcliffe Efficiency (NSE), and percentage bias (PBIAS) to evaluate the model performance.

The optimal model performance was achieved with a melt threshold temperature (T_M) of -2.45°C and a precipitation gradient (Pg) of 88% km^{-1}, which resulted in the lowest RMSE of 27.65 m^3/s during the calibration period 2000–2002 for the Gangotri Glacier system.

Additionally, the statistical analysis, like the coefficient of determination (R^2), Nash–Sutcliffe Efficiency (NSE), and Percent Bias (PBIAS) to evaluate the performance of the model. These indicators were computed using the following equations.

$$RMSE = \sqrt{\frac{\sum_{i=1}^{n}(Q_{sim}-Q_{obs})^2}{n}} \quad (9)$$

$$R^2 = \left(\frac{\sum_{i=1}^{n}(Q_{obs}-\bar{Q}_{obs}).(Q_{sim}-\bar{Q}_{sim})}{\sqrt{\sum_{i=1}^{n}(Q_{obs}-\bar{Q}_{obs})^2.\sum_{i=1}^{n}(Q_{sim}-\bar{Q}_{sim})^2}} \right)^2 \quad (10)$$

$$NSE = 1 - \left\{ \frac{\sum_{i=1}^{n}(Q_{obs}-Q_{sim})^2}{\sum_{i=1}^{n}(Q_{obs}-\bar{Q}_{obs})^2} \right\} \quad (11)$$

$$PBIAS = \frac{\sum_{i=1}^{n}(Q_{sim}-Q_{obs})}{\sum_{i=1}^{n} Q_{obs}} \times 100 \quad (12)$$

4.4 Model Validation

The model output was validated using in situ runoff from the Bhojbasa runoff station for the year 2003. The model was run using the calibrated parameters: T_M of –2.45°C and Pg of 88% per kilometre.

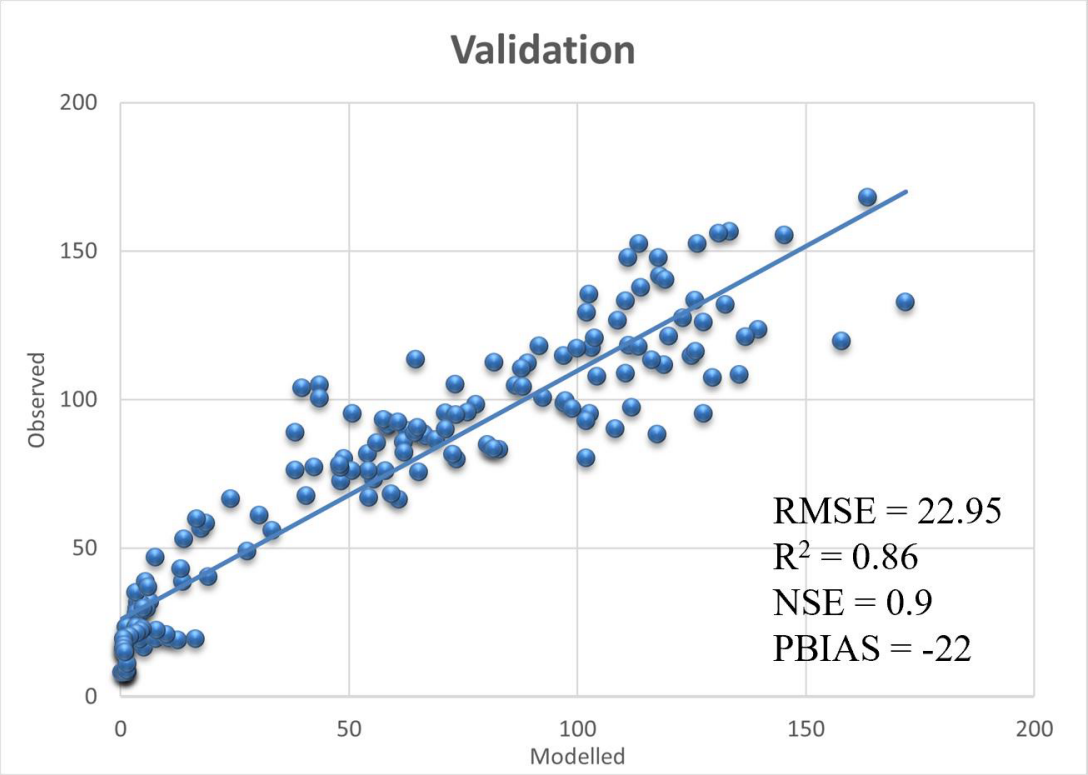

Figure 5: Validation scatter plot comparing modelled and observed runoff for the Gangotri Glacier basin. The plot includes performance metrics such as coefficient of determination (**R^2**), root mean square error (**RMSE**), Nash–Sutcliffe Efficiency (**NSE**), and percentage bias (**PBIAS**) to assess the accuracy and reliability of the model during the validation period.

These performance metric values, which are shown above (Figure 5), indicate that the model performed exceptionally well during the validation period, with strong predictive capability and minimal deviation from observed data. The results showed a reasonable match between simulated and observed runoff, indicating that the model could effectively capture seasonal variations and the general runoff response during the melt season. Some differences were noted during the early melt period and peak flow days.

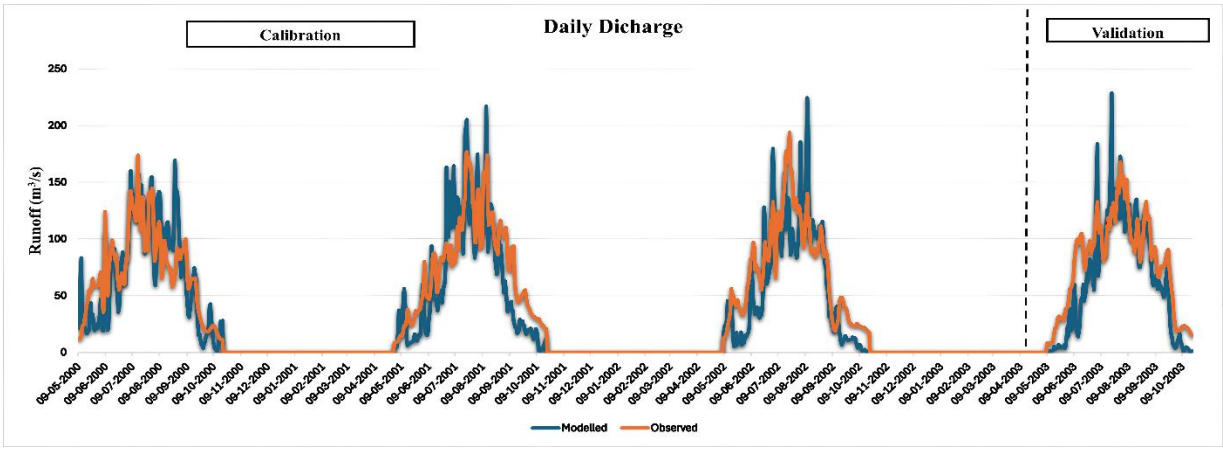

Figure 6: Line graph between modelled and observed runoff

4.5 Model Sensitivity

To assess the model's sensitivity, basin-wide runoff was estimated by re-running the model by varying each parameter, keeping other parameters constant. Degree day factor for snow, ice, and debris-covered ice is altered by ±1 $mmd^{-1}°C^{-1}$, and for the threshold temperature of melt (T_M) and precipitation gradient (P_G), it is altered by ±10% respectively. Runoff sensitivities were evaluated for the period spanning 1980 to 2020 using this equation

$$\frac{dtotr}{di} = \frac{totr(i_H) - totr(i_L)}{2} \quad (13)$$

Where totr is the average annual total runoff over the period 1980-2020, i_H is the highest value of the parameter, and $i_L$is the lowest value of the parameter.

Chapter 5: Results

5.1 Annual Runoff Variability (1980-2020)

An analysis of simulated runoff data for the GGS between 1980 and 2020 reveals notable interannual variability (Figure 7). The average total annual runoff during this period was approximately 29.27 m^3/s. The highest runoff of 33.34 m^3/s was observed in 1994. On the other hand, the lowest runoff was recorded in 1989, with only 24.37 m^3/s (Figure 7).

The mean annual snow runoff is 10.57 m^3/s over the whole period. The maximum snow runoff was observed in 2013, reaching 12.66 m^3/s. The minimum snow runoff occurred in 2004, with a value of 7.90 m^3/s. However, the ice runoff exhibited an annual mean of 15.2 m^3/s, making it the dominant contributor to total runoff with the highest ice runoff of 19.56 m^3/s and the lowest ice runoff of 11.37 m^3/s in the years 2016 and 1982, respectively. For the period **1980-2020**, **ice runoff** contribution is dominating, i.e**., 52%,** and snow **runoff** and **rain runoff** contributions are **36%** and **12%,** respectively.

The analysis of annual climatic variables over the study period revealed notable interannual variability in both precipitation and temperature. The average annual precipitation was recorded as 493.18 mm, with the maximum value of 621.79 mm occurring in the year 2019, and the minimum value of 374.49 mm observed in 2001. In terms of temperature, the average annual temperature across the study period was 1.90°C. The highest average temperature of 3.26°C was recorded in 2016, whereas the lowest, 0.62°C, was observed in 1997.

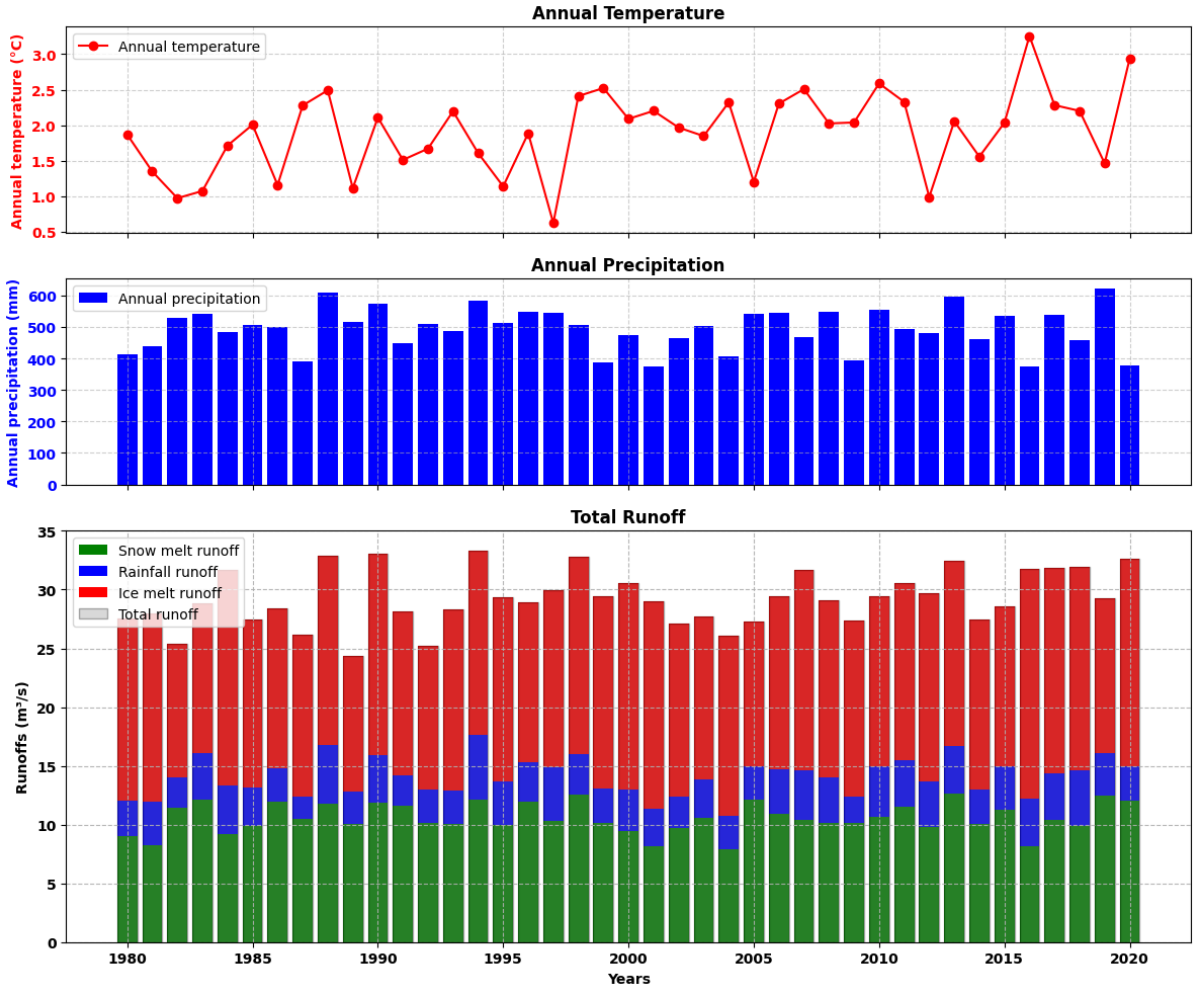

Figure 7: Presents the interannual variability of total runoff from the GGS between 1980 and 2020, along with corresponding changes in mean annual temperature and total precipitation

5.2 Changes in Runoff Behaviour: Pre-2000 and post-2000

To assess long-term changes in runoff patterns, the dataset was divided into two periods: pre-2000 (1980–2000) and post-2000 (2001–2020). A comparative analysis was conducted for the major runoff components—snow runoff, ice runoff, and total runoff—to evaluate the hydrological shifts in the GGS over time. During the pre-2000 period, the average total runoff was approximately 29.03 m^3/s, whereas in the post-2000 period, it increased to 29.57 m^3/s.

A more detailed examination reveals that ice runoff increased noticeably, from 14.89 m^3/s (pre-2000) to 15.53 m^3/s (post-2000). In contrast, snow runoff slightly declined, from an average of 10.67 m^3/s before 2000 to 10.45 m^3/s after 2000.

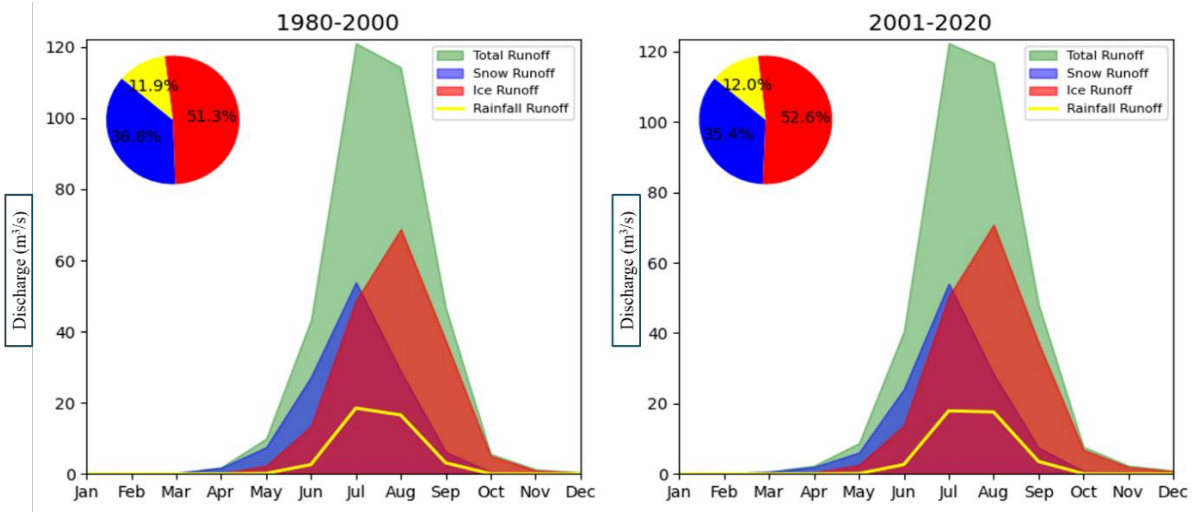

Figure 8: Illustrates the seasonal hydrographs of the GGS for two time periods: 1980–2000 and 2001–2020. The hydrographs display the monthly variation in total runoff and its contributing components—snow runoff, ice runoff, and rainfall runoff. Each hydrograph is accompanied by a pie chart showing the average percentage contribution of each component to total runoff during the respective period.

In both periods, runoff follows a seasonal pattern, rising quickly from May, reaching a peak in July and August, and then decreasing by October (Figure 8). During the 1980–2000 period, ice runoff accounted for approximately 51.3% of the total annual runoff, snow runoff contributed 36.8%, and rainfall runoff made up 11.9%. In the 2001–2020 period, ice runoff contribution increased slightly to 52.6%, while snow runoff decreased to 35.4%. The share of rainfall-runoff remained nearly constant at 12%. This shift indicates a gradual transition toward a more ice-dominated runoff regime. The observed increase in ice runoff contribution, along with visual patterns in the seasonal hydrograph, also points toward a shift in the timing of runoff generation. Specifically, recent years show signs of earlier melt onset, with measurable runoff beginning well before the typical start of the ablation season. To explore this further, the following section examines the trend of early-season melt, particularly focusing on runoff contributions occurring before April.

5.3 Early Melt Onset and Season Runoff Contribution

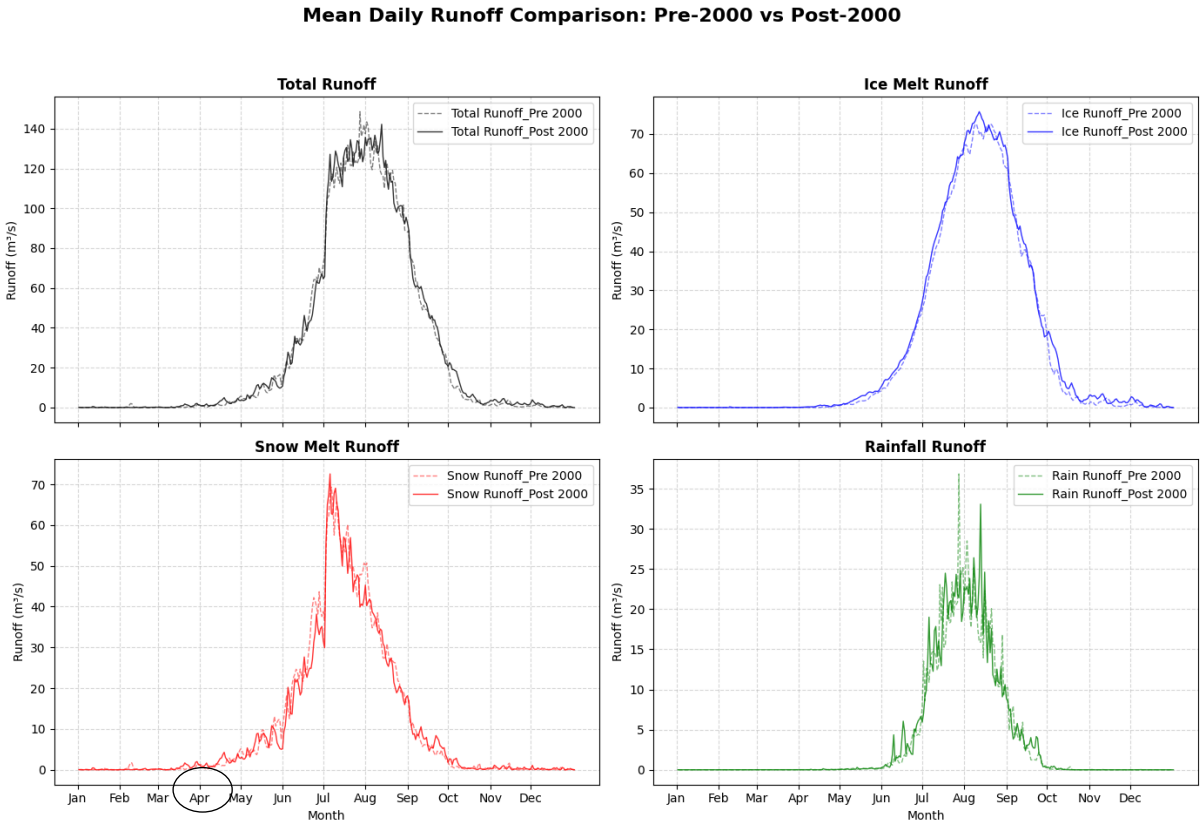

Figure 9: Shows the monthly variation in runoff components—snow runoff, ice runoff, rainfall-runoff, and total runoff—for two distinct periods: 1980–2000 (pre-2000) and 2001–2020 (post-2000). A clear shift is evident in the timing of runoff initiation, especially for snow runoff.

In the post-2000 period, the onset of mean monthly snow runoff begins as early as April, whereas in the pre-2000 period, significant snow runoff activity typically starts closer to May. The mean temperature during February and March has increased from –4.73 °C in the pre-2000 period to –4.10 °C in the post-2000 period, indicating a warming of approximately 0.6 °C. This observed increase in early spring temperature supports the earlier onset of snow and runoff seen in the model simulations after 2000 (see Figure 9). Warmer pre-monsoon temperatures appear to be triggering earlier seasonal melting, particularly of low-lying snow cover, resulting in runoff generation earlier in the year.

The total runoff curve for the post-2000 period also begins to rise earlier, following the earlier snow runoff trend. However, the snow component still dominates during the peak melt season in July–August. Rainfall-runoff patterns show similar seasonal behaviour across both periods but contribute slightly more during the post-monsoon months in the post-2000 period.

Chapter6: Discussion

6.1 Trend analysis of climate parameters and runoff

In this study, long-term trends in key hydrometeorological variables and runoff components in the Gangotri Basin were analysed using the Mann-Kendall test and Sen's slope estimator over the period 1980–2020.

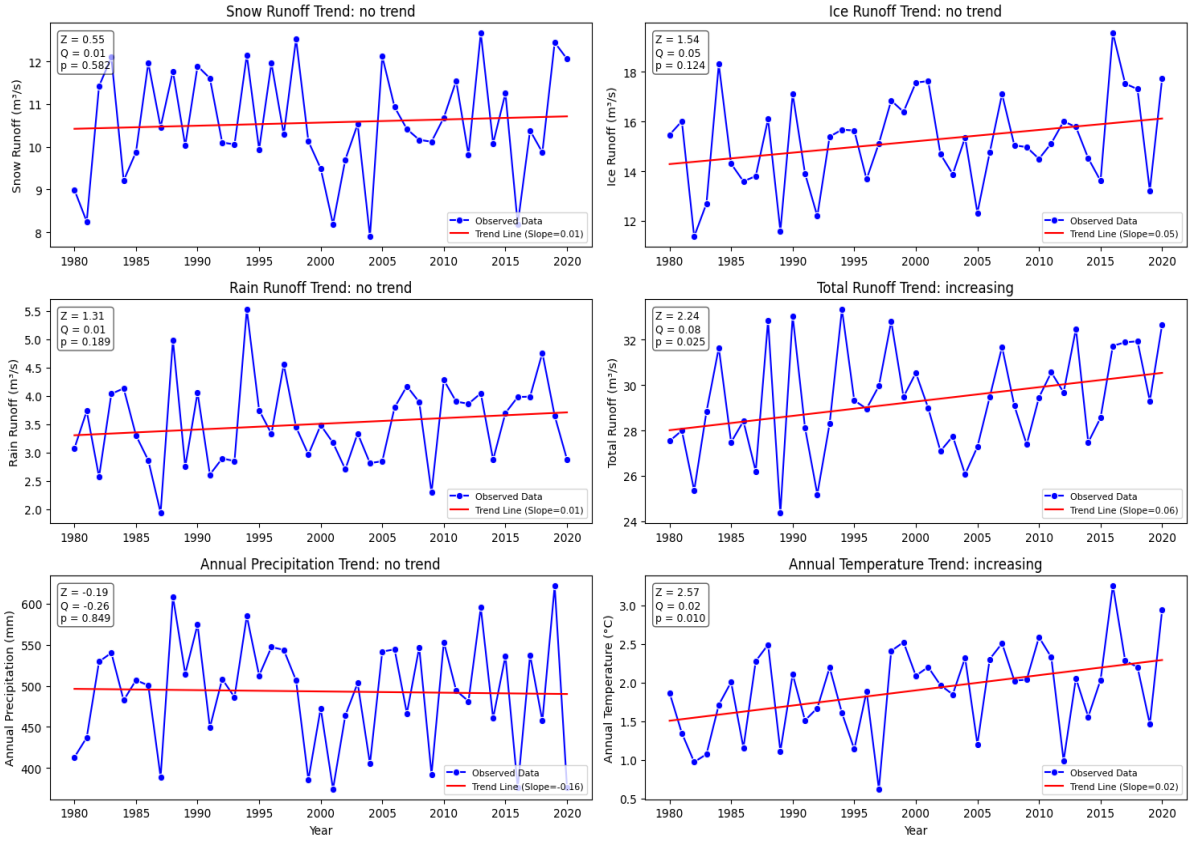

Figure 10: Trends in mean annual temperature, precipitation, and various hydrological components in the Gangotri Basin during the period 1980–2020.

The Z-value in the Mann-Kendall test is a standardized statistic that reflects both the direction and magnitude of a trend, where positive values signify an upward trend and negative values indicate a downward trend. Trends are considered statistically significant when the absolute Z-value exceeds a specific threshold. Common thresholds include $|Z| > 1.645$ for significance at the 10% level, $|Z| > 1.96$ for 5%, and $|Z| > 2.576$ for 1% significance (Mann, 1945; Kendall, 1975; Gilbert, 1987). In our case, we have used a 5% significance level value for measuring of strength of the trend. The Q-value, also known as Sen's slope estimator, measures the trend's magnitude and is calculated as the median of all possible pairwise slopes. A positive Q-value suggests an increasing trend, while a negative one indicates a decreasing trend. The p-value represents the probability that the observed trend is due to random chance; a p-value below

0.10 is typically considered statistically significant at the 10% level. Z-values are dimensionless, Q-values are in the units of the analyzed variable, and p-values range from 0 to 1. The analysis reveals a statistically significant increasing trend in annual temperature, with a Z-value of 2.572, a Sen's slope of 0.02 °C/year, and a p-value of 0.010. This rising temperature trend is consistent with broader regional warming patterns observed in the Western Himalaya. Over the period, annual precipitation did not show any clear increasing or decreasing trend (Z = –0.191, Q = –0.259, p = 0.849). This suggests that precipitation varied from year to year without any consistent pattern or long-term directional change.

Among the hydrological components, total runoff exhibits a significant positive trend (Z = 2.235, Q = 0.076, p = 0.025), indicating a gradual increase in annual water yield from the basin. This increase in runoff, despite the absence of a significant precipitation trend, suggests a strong temperature-driven influence on runoff generation processes.

Further runoff components show that ice, snow, and rain runoff all demonstrate mild increasing trends based on their Sen's slope values (0.049, 0.009, and 0.011, respectively). However, the trends for ice runoff, snow runoff, and rain runoff are all statistically insignificant, with corresponding p-values of 0.124, 0.582, and 0.189, respectively.

The increasing runoff is likely a response to higher temperatures that enhance snow and ice runoff, even in the absence of increased rainfall. This is in line with earlier studies conducted in Chhota Shigri glacier and the upper Indus basin, which report similar patterns of rising temperatures and associated increases in glacier and snow runoff contributions (e.g., Azam et al., 2014; Immerzeel et al., 2009). While precipitation remains highly variable and statistically insignificant, warming temperatures accelerate melt processes, thereby increasing runoff. Although this increase in water availability may appear beneficial in the short term, it raises long-term concerns regarding glacier mass balance and future water security, especially as glacier volumes continue to decline under sustained warming.

6.2 Climate driver of runoff dynamics

Due to the limited availability of long-term in-situ runoff data in the Himalayan region, particularly in remote basins, understanding the climatic controls on runoff generation remains a significant challenge. Only a few studies have explored the climatic influence on hydrology in glacierized catchments, often restricted to small-scale or glacier-specific analyses (e.g., Srivastava and Azam, 2022a; Laha et al., 2023; Singh et al., 2023a). To better understand the dominant climatic drivers of runoff variability at the basin scale, correlation coefficients (r)

were calculated between annual and seasonal climatic parameters and different hydrological components over the study period (Fig. 11).

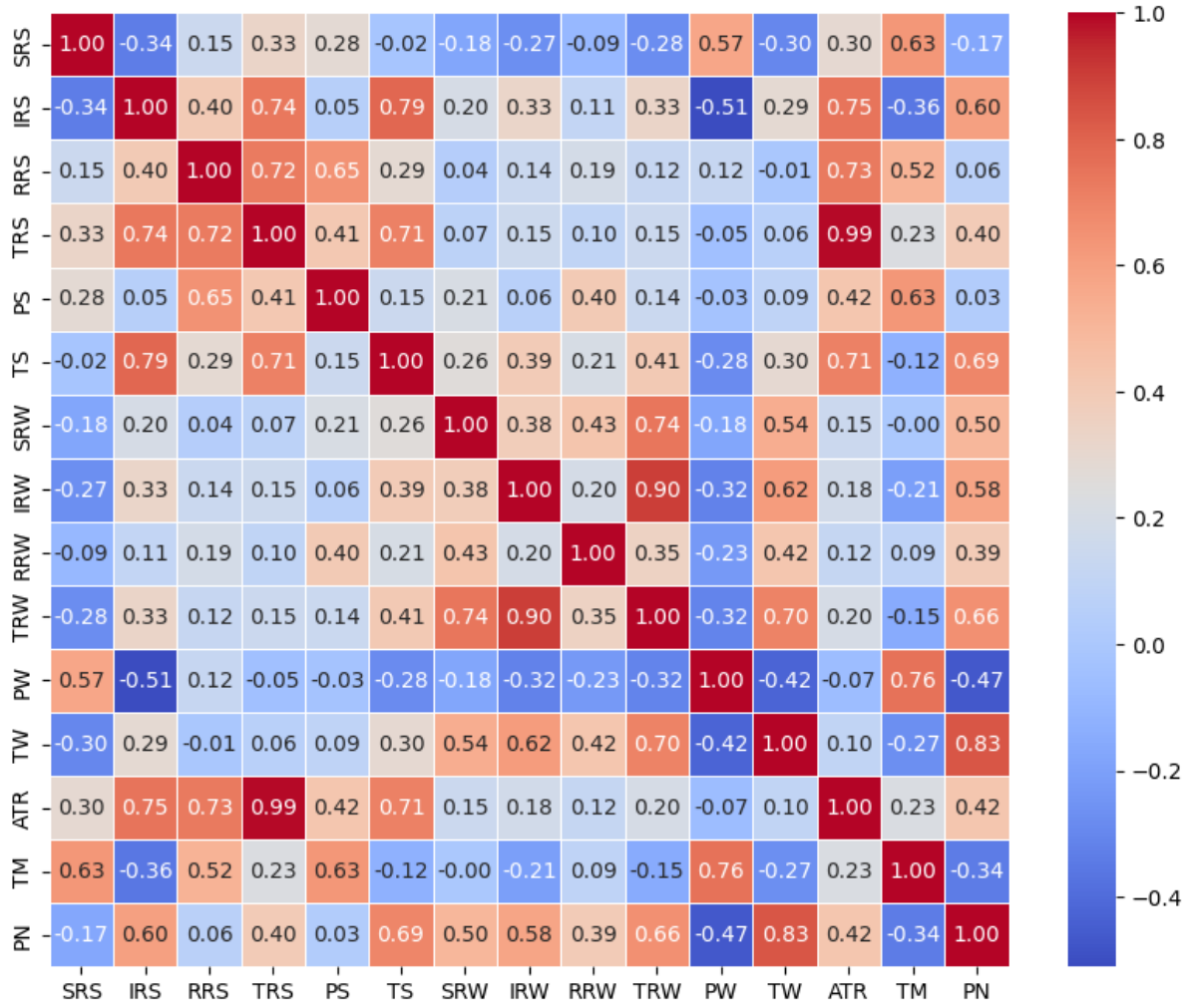

Figure 11: Correlation matrix for the Gangotri Basin.PS, PW, PN = Summer, winter, and annual precipitation, respectively; TS, TW, TM = Summer, winter, and annual temperature, respectively; TRS, TRW, TRM = Summer, winter, and annual total runoff, respectively; RRS, RRW, RRM = Summer, winter, and annual rainfall-runoff, respectively; SRS, SRW, SRM = Summer, winter, and annual snow runoff, respectively; IRS, IRW, IRM = Summer, winter, and annual ice runoff, respectively; ATR = Annual total runoff.

The total runoff summer (TRS) shows the strongest positive correlations with annual total runoff (ATR; r = 0.99) and summer temperature (TS; r = 0.95), highlighting the dominant role of summer temperature in regulating meltwater contributions from both snow and glaciers. Moderate-to-strong positive correlations are also observed between TRS and summer precipitation (PS; r = 0.65) and with PN (annual precipitation; r = 0.69), indicating that both snow and rainfall events contribute to runoff volumes.

The summer ice runoff (IRS) shows a strong correlation with summer temperature (TS; r = 0.79) and summer total runoff (TRS; r = 0.74), highlighting that ice runoff is highly sensitive to seasonal temperature fluctuations. Ice runoff also shows a moderate positive correlation with annual precipitation (PN; r = 0.60), as higher snowfall increases glacier mass, which later contributes to greater ice runoff during the ablation season. Snow runoff in summer (SRS) shows a weak correlation with summer temperature (TS: r = 0.28) and annual temperature (ATR: r = 0.33), as well as with summer total runoff (TRS: r = 0.33) and summer precipitation (PS: r = 0.28). These weak correlations indicate that snow runoff is more influenced by the availability of fresh snowfall rather than by direct temperature increases, particularly during the early part of the melt season. Rain runoff summer (RRS) and its seasonal counterparts (RRW, IRW, TRW) are moderately to strongly correlated with PS (r = 0.65–0.72) and temperature variables (TS, TM; r ≈ 0.60–0.70), indicating the combined influence of both seasonal and annual rainfall intensity and temperature on the runoff component. Notably, RRW and TRW show high correlations with PN (r = 0.58–0.66), confirming their dependence on precipitation variability.

Annual total runoff (ATR) is highly correlated with most runoff components and temperature, including TRS (r = 0.99), TS (r = 0.95), and TM (r = 0.75), establishing summer temperature as the primary driver of hydrological response in this basin. This aligns with earlier findings in other Himalayan basins where summer or annual mean temperature was a key control on runoff generation (Singh et al., 2000; Immerzeel et al., 2009; Arora et al., 2014).

The correlation matrix shows that summer temperature (TS) strongly influences both ice runoff and total runoff, while summer precipitation (PS) and annual precipitation (PN) mainly affect snow and rain runoff components. For annual total runoff (ATR), summer temperature is identified as the main controlling factor, with additional influence from summer and annual precipitation.

6.4 Model sensitivity

A sensitivity analysis was carried out to assess the impact of individual model parameters on modelled basin-wide runoff. Each parameter was varied while keeping all other inputs constant (equation 13). This analysis helps to identify which parameters exert the greatest influence on model outputs.

Two approaches were used to vary the parameters:

- For the threshold temperature for melt (T_M) and altitudinal precipitation gradient (Pg), the values were varied from ±10% of their calibrated values, respectively.
- For degree-day factors (DDFs) were varied by ±1 mm d^{-1} $°C^{-1}$ to check the DDF sensitivity.

Table 3: Sensitivity of simulated total runoff to variations in key glacio-hydrological model parameters. For T_M (threshold temperature for melt) and Pg (altitudinal precipitation gradient), sensitivity was evaluated by varying parameter values by ±10% from their calibrated values. For degree-day factors (DDF) of snow, clean ice, and debris-covered ice, a fixed step change of ±1 mm d^{-1} $°C^{-1}$ was applied.

Parameters	Model Value	Highest Value	Lowest Value	Sensitivity (m^3/s)
DDF for debris-covered ice (mm d^{-1} $°C^{-1}$)	4.5	3.5	5.5	1.45
DDF for ice (mm d-1 $°C^{-1}$)	7.7	6.7	8.7	1.13
DDF for snow (mm d^{-1} $°C^{-1}$)	6.1	5.1	7.1	1.52
Altitudinal precipitation gradient Pg(%km^{-1})	88	79.2	96.8	0.25
Threshold temperature for melting (T_M)	-2.45	-2.205	-2.695	2.17

The resulting sensitivities, calculated as the total change in average annual runoff based on the simulations, are shown in Table 5. The model identified the threshold temperature for melt (T_M) as the most sensitive parameter, with a sensitivity value of 2.17 m^3/s. This is because T_M determines the onset of melting; even small changes in this threshold can shift when melting begins, significantly affecting the volume and timing of runoff. Among the degree-day factors (DDF), snow showed the highest sensitivity (1.52), followed by debris-covered ice (1.45) and clean ice (1.13). These parameters control how much melt occurs per degree of temperature above TM, making them critical for accurately simulating the magnitude and timing of meltwater runoff

The high sensitivity to snow DDF (1.52) shows that snow runoff plays a big role in overall runoff. Even small changes in this value can lead to noticeable changes in modelled streamflow, especially with changing temperature and snowfall.

In contrast, the altitudinal precipitation gradient (Pg) had the lowest sensitivity (0.25) because changes in precipitation distribution with elevation have a smaller impact on runoff compared to temperature-driven melt processes, especially in glacier-dominated basins where melt governs most of the runoff.

6.5 Limitation of Study

Despite offering valuable insights into the climatic sensitivity and runoff behaviour of the Gangotri Glacier basin, the current study has several inherent limitations. One significant constraint is the absence of radiation components in the melt simulation process. The glacio-hydrological model used in this study employs a degree-day approach, which does not explicitly incorporate radiative energy fluxes such as shortwave and longwave radiation. Consequently, critical surface energy balance controls, such as albedo variations, cloud cover influence, and surface radiation interactions, are not represented, thereby limiting the physical accuracy of the melt simulations.

Additionally, the model operates on elevation bands rather than a grid-based (spatially distributed) framework, which reduces its ability to capture spatial variability in meteorological inputs, land surface properties, and glacier response across the catchment. This limitation hinders the model's effectiveness in identifying localised runoff dynamics or sub-catchment heterogeneity, which are especially important in complex mountainous terrain.

Another notable limitation is the exclusion of evapotranspiration (ET) processes. In the current setup, ET losses are not considered, even though they may constitute a significant component of the water balance, particularly in non-glacierized and lower-elevation zones during the melt season. The absence of ET may result in a slight overestimation of runoff, especially during the warmer months.

Lastly, the model incorporates a simplified representation of snow and ice runoff using fixed degree-day factors (DDF) for snow, clean ice, and debris-covered ice. This approach assumes uniform melt behaviour and does not account for dynamic factors such as varying debris thickness, changing surface albedo, and local meteorological influences within the ablation zone. These simplifications, while necessary for model efficiency and data constraints, introduce uncertainties in the spatial and temporal distribution of melt and runoff outputs.

Chapter 7: Conclusion and scope of future work

This study presents a comprehensive assessment of climatic and hydrological changes in the Gangotri Glacier basin using a glacial modelling approach from 1980 to 2020. The average total annual runoff over the period 1980-2020 was approximately 29.27 m^3/s. The highest runoff of 33.34 m^3/s was observed in 1994. On the other hand, the lowest runoff was recorded in 1989, with only 24.37 m^3/s. The analysis also reveals a slight increase in total runoff, rising from an average of 28.96 m^3/s during the pre-2000 period to 29.57 m^3/s after 2000. This change is primarily attributed to a notable increase in ice runoff, which rose from 14.76 m^3/s to 15.63 m^3/s, indicating intensified glacier melt in response to increased warming. In contrast, snow runoff showed a minor decline, possibly due to shifting snowfall patterns, reduced snow accumulation, or earlier seasonal melting caused by rising temperatures. The proportional contribution of runoff components also changed over time. The share of ice runoff increased from 51.3% to 52.6%, while snow runoff contribution declined from 36.8% to 35.4%. Rainfall-runoff remained relatively stable, increasing only slightly from 11.9% to 12.0% between the two periods. Despite these changes, ice runoff remained the dominant contributor to total runoff in both pre- and post-2000 periods.

The trend analysis revealed a statistically significant increase in mean annual air temperature over the period 1980–2020, while precipitation did not show a clear trend. Despite this, total runoff exhibited a positive trend, indicating that temperature-driven processes, especially snow and ice runoff, play a dominant role in controlling water availability in this glacier-fed basin. The increasing temperature trend was also reflected in the observed earlier onset of snow runoff and total runoff, with melt initiation advancing from May (pre-2000) to April (post-2000), highlighting that warming occurs during late winter and early spring months.

The correlation matrix shows that summer temperature (TS) strongly influences both ice runoff and total runoff, while summer precipitation (PS) and annual precipitation (PN) mainly affect snow and rain runoff components. For annual total runoff (ATR), summer temperature is identified as the main controlling factor. The correlation analysis further supported these observations, showing strong positive relationships between temperature variables and total/ice runoff components, while precipitation was more closely linked with snow and rain runoff. The threshold temperature for melting (T_M) was found to be the most sensitive parameter with a sensitivity of 2.17, followed by the degree-day factors (DDF) for snow, debris-covered ice, and

clean ice with the sensitivities of 1.52, 1.45, and 1.13, respectively. In contrast, the altitudinal precipitation gradient exhibited a minimum sensitivity of 0.25m^3/s.

This study contributes to a better understanding of the hydrological components of one of the largest glacier basins in the central Himalaya and provides a framework for runoff assessment that can help in the planning and management of future water resources.

Although this study provides significant insights into runoff dynamics and their climatic drivers, future research could explore several important dimensions. Incorporating more detailed representations of glacier dynamics, such as ice flow modelling and supraglacial hydrology, could improve the simulation of glacier melt contributions. Future work should also consider the impacts of debris cover variation and black carbon deposition on melt rates, as these are known to influence glacier energy balance. Moreover, integrating higher-resolution remote sensing data and expanding field-based validation of snow and glacier mass balance would further enhance model accuracy. Long-term projections under different climate scenarios using regional climate models (RCM_S) could be employed to assess future water availability and support regional water resource planning and disaster preparedness in the context of increasing climate variability.

REFERENCES

- Azam, M. F., & Srivastava, S. (2020). Mass balance and runoff modelling of partially debris-covered Dokriani Glacier in monsoon-dominated Himalaya using ERA5 data since 1979. Journal of Hydrology, 590, 125432.
- Azam, M. F., Ramanathan, A. L., Wagnon, P., Vincent, C., Linda, A., Berthier, E., … Pottakkal, J. G. (2016). Meteorological conditions, seasonal and annual mass balances of Chhota Shigri Glacier, western Himalaya, India. Annals of Glaciology, 57(71), 328–338. doi:10.3189/2016AoG71A570
- Azam, M. F., Wagnon, P., Vincent, C., Ramanathan, A. L., Kumar, N., Srivastava, S., Pottakkal, J. G., & Chevallier, P. (2019). Snow and ice runoff contributions in a highly glacierized catchment of Chhota Shigri Glacier (India) over the last five decades. Journal of Hydrology, 574, 760-77
- Bhambri, R., Bolch, T., & Chaujar, R. K. (2012). Frontal recession of Gangotri Glacier, Garhwal
- Bolch, T., Kulkarni, A., Kaab, A., Huggel, C., Paul, F., Cogley, J. G., ... & Stoffel, M. (2012). The state and fate of Himalayan glaciers. Science, 336(6079), 310–314. https://doi.org/10.1126/science.1215828
- Bolch, T., Kulkarni, A., Kaab, A., Huggel, C., Paul, F., Cogley, J. G., ... & Stoffel, M. (2019). The state and fate of Himalayan glaciers. Science, 336(6079), 310-314.
- Bolch, T., Kulkarni, A., Kääb, A., Huggel, C., Paul, F., Cogley, J. G., Frey, H.,Kargel, J. S., Fujita, K., Scheel, M., & Bajracharya, S. (2012). The state and fate of Himalayan glaciers. Science, 336(6079), 310–314.
- Chaturvedi, S., Cheong, T. S., Luo, Y., Singh, C., & Shaw, R. (2022). IPCC Sixth Assessment Report (AR6): Climate Change 2022—Impacts, adaptation and vulnerability: Regional factsheet asia. Retrieved June 5, 2022, from https://policycommons.net/artifacts/2264289/ipcc_ ar6_wgii_factsheet_asia/3023343/ CID: 20.500.12592/sc4xfx
- Chen, X., Long, D., Hong, Y., Zeng, C., Yan, D., 2017. Improved modelling of snow and glacier melting by a progressive two-stage calibration strategy with GRACE and multisource data: How snow and glacier meltwater contribute to the runoff of the Upper Brahmaputra River basin. Water Resour. Res. 53, 2431–2466. https://doi.org/ 10.1002/2016wr019656.

- Gantayat, P., Kulkarni, A. V., & Srinivasan, J. (2014). Estimation of ice thickness using surface velocities and slope: case study at Gangotri Glacier, India. Journal of Glaciology, 60(220), 277–282. doi:10.3189/2014JoG13J078
- Gardelle, J., Berthier, E., Arnaud, Y., Kaab, A., 2013. Region-wide glacier mass balances over the Pamir-Karakoram-Himalaya during 1999–2011 (vol 7, pg 1263, 2013). Cryosphere 7 (6), 1885–1886. https://doi.org/10.5194/tc-7-1263-2013.
- Gilbert, R.O. 1987. Statistical Methods for Environmental Pollution Monitoring. Wiley, New York.
- Hasnain, S. I. (1999). Himalayan glaciers: hydrology and hydrochemistry. Allied Publishers.
- Hersbach, H., Bell, B., Berrisford, P., Hirahara, S., Horányi, A., Muñoz-Sabater, J., ... & Thépaut, J. N. (2020). The ERA5 global reanalysis. Quarterly journal of the royal meteorological society, 146(730), 1999-2049.
- Himalaya, from 1965 to 2006, measured through high-resolution remote sensing data. Current Science, 102(3), 489-494.
- Hock, R., 2003. Temperature index melt modelling in mountain areas. J. Hydrol. 282 (1–4),104–115.https://doi.org/10.1016/S0022-1694(03)00257-9.
- Huss, M., & Hock, R. (2018). Global-scale hydrological response to future glacier mass loss. Nature Climate Change, 8(2), 135–140.
- Hussain, M. A., Azam, M. F., Srivastava, S., & Vinze, P. (2022). Positive mass budgets of high-altitude and debris-covered fragmented tributary glaciers in the Gangotri Glacier System, Himalaya. Frontiers in Earth Science, 10, 978836.
- Hussain, M. A., Azam, M. F., Srivastava, S., & Vinze, P. (2022). Positive mass budgets of high-altitude and debris-covered fragmented tributary glaciers in the Gangotri Glacier System, Himalaya. Frontiers in Earth Science, 10, 978836. https://doi.org/10.3389/feart.2022.978836
- Immerzeel, W. W., van Beek, L. P. H., Konz, M., Shrestha, A. B., & Bierkens, M. F. P. (2012). Hydrological response to climate change in a glacierized catchment in the Himalaya. Climatic Change, 110(3–4), 721–736. https://doi.org/10.1007/s10584-011-0143-4
- Kääb, A., Berthier, E., Nuth, C., Gardelle, J., Arnaud, Y., 2012. Contrasting patterns of early twenty-first-century glacier mass change in the Himalaya. Nature 488 (7412),495–498. https://doi.org/10.1038/nature11324
- Kendall, M.G. 1975. Rank Correlation Methods, 4th Edition. Charles Griffin, London.

- Khanal, S., Lutz, A. F., Kraaijenbrink, P. D., van den Hurk, B., Yao, T., & Immerzeel, W. W. (2021). Variable 21st century climate change response for rivers in High Mountain Asia at seasonal to decadal time scales. Water Resources Research, 57(5), e2020WR029266.
- Lutz, A. F., Immerzeel, W. W., Shrestha, A. B., & Bierkens, M. F. P. (2014). Consistent increase in High Asia's runoff due to increasing glacier melt and precipitation. Nature Climate Change, 4(7), 587–592. https://doi.org/10.1038/nclimate2237
- Mann, H.B. 1945. Non-parametric tests against trend. Econometrica 13, 163-171.
- Mohd. Farooq Azam et al., Glaciohydrology of the Himalaya Karakoram.Science373, eabf3668(2021). DOI:10.1126/science.abf3668
- Nakawo, M., Fujita, K., Ageta, U., Shankar, K., Pokhrel, P. A., & Tandong, Y. (1997). Basic studies for assessing the impacts of the global warming on the Himalayan cryosphere. Bull Glacier Res, 15, 53-58.
- Nepal, S., Krause, P., Flügel, W.A., Fink, M., Fischer, C., 2014. Understanding the hydrological system dynamics of a glaciated alpine catchment in the Himalayan region using the J2000 hydrological model. Hydrol. Process 28, 1329–1344. https://doi.org/10.1002/hyp.9627.
- Nie, Y., Pritchard, H. D., Liu, Q., Hennig, T., Wang, W., Wang, X., Liu, S.,Nepal, S., Samyn, D., Hewitt, K., & Chen, X. (2021). Glacial change and hydrological implications in the Himalaya and Karakoram. Nature Reviews Earth & Environment, 2(2), 91–106.
- Nuimura, T., Sakai, A., Taniguchi, K., Nagai, H., Lamsal, D., Tsutaki, S., et al. (2015). The GAMDAM Glacier Inventory: A quality-controlled inventory of asian glaciers. Cryosphere 9 (3), 849–864. doi:10.5194/tc-9-849-2015
- Oerlemans, J., Giesen, R. H., & van den Broeke, M. R. (2009). Retreating alpine glaciers: increased melt rates due to accumulation of dust (Vadret da Morteratsch, Switzerland). Journal of Glaciology, 55(192), 729–736. https://doi.org/10.3189/002214309789470969
- Racoviteanu, A.E., Armstrong, R., Williams, M.W., 2013. Evaluation of an ice ablation model to estimate the contribution of melting glacier ice to annual runoff in the Nepal Himalaya. Water Resour. Res. 49, 5117–5133. https://doi.org/10.1002/wrcr.20370.
- Rai, S.P., Thayyen, R.J., Purushothaman, P., Kumar, B., 2016. Isotopic characteristics of cryospheric waters in parts of Western Himalaya, India. Environ. Earth Sci. 75 (7),600. https://doi.org/10.1007/s12665-016-5417-8.

- Shea, J. M., Immerzeel, W. W., Wagnon, P., Vincent, C., & Bajracharya, S. (2015). Modelling glacier change in the Everest region, Nepal Himalaya. The Cryosphere, 9(3), 1105–1128. https://doi.org/10.5194/tc-9-1105-2015

- Shea, J. M., Immerzeel, W. W., Wagnon, P., Vincent, C., & Bajracharya, S. (2015). Modelling glacier change in the Everest region, Nepal Himalaya. The Cryosphere, 9(3), 1105–1128. https://doi.org/10.5194/tc-9-1105-2015

- Singh, D. S., Singh, A. K., Dubey, C. A., Kumar, D., Sangode, S. J., Trivedi, A., ... & Singh, J. (2022). Multi-Proxy analysis in the Gangotri Glacier region, Garhwal Himalaya: Glacial Stratigraphy and the overview of snout retreat, geomorphic evolution, and palaeoclimate signatures. Journal of the Palaeontological Society of India, 67(1), 158-182.
- Singh, J., Singh, V., Ojha, C. S. P., & Arora, M. K. (2023). Assessment of recent changes (2011–2020) in glacier thickness and runoff variability in Gangotri glacier, India. Hydrological Sciences Journal, 68(15), 2223-2242.
- Singh, J., Vishal, S., Ojha, C. S. P., & Arora, M. K. (2023). Assessment of recent changes (2011–2020) in glacier thickness and runoff variability in Gangotri Glacier, India. Hydrological Sciences Journal, 68(15), 2223–2242. https://doi.org/10.1080/02626667.2023.2240190
- Singh, J., Vishal, S., Ojha, C. S. P., & Arora, M. K. (2023). Assessment of recent changes (2011–2020) in glacier thickness and runoff variability in Gangotri Glacier, India. Hydrological Sciences Journal, 68(15), 2223-2242.
- Singh, P., Arora, M., & Goel, N. K. (2006). Effect of climate change on runoff of a glacierized Himalayan basin. Hydrological Processes, 20(9), 1979–1992. https://doi.org/10.1002/hyp.5991
- Singh, P., Haritashya, U.K., Kumar, N., & Singh, Y. (2006). Hydrological characteristics of the Gangotri glacier, central Himalaya, India. Journal of Hydrology, 327(1-2), 55-67.
- Singh, V., Jain, S. K., & Shukla, S. (2021). Glacier change and glacier runoff variation in the Himalayan Baspa River basin. Journal of Hydrology, 593, 125918.
- Thayyen, R.J., Gergan, J.T., 2010. Role of glaciers in watershed hydrology: a preliminary study of a“ Himalayan catchment”. Cryosphere 4 (1), 115–128. https://doi.org/10.5194/tc-4-115-2010.

- Wadia Institute of Himalayan Geology. (2024). Long-term monitoring of Gangotri Glacier, Garhwal Himalaya. Annual Report (April 2023 - March 2024), Uttarakhand State Disaster Management Authority.
- Wagnon, P., Linda, C., Azam, M. F., Vincent, C., & Ramanathan, A. L. (2013). Seasonal and annual mass balances of Chhota Shigri Glacier, western Himalaya, India, since 2002. The Cryosphere, 7(2), 569–582. https://doi.org/10.5194/tc-7-569-2013